Optik - International Journal for Light and Electron Optics 246 (2021) 167797

Contents lists available at ScienceDirect

Optik

journal homepage: www.elsevier.com/locate/ijleo

Study of gas dynamics in hollow-core photonic crystal fibers

Yan Li, Xuemei Yang, Xiangying Hao, Shun Wu *

Hubei Key Laboratory of Optical information and Pattern Recognition, Wuhan Institute of Technology, Wuhan 430205, China

ARTICLE INFO

Keywords:
Hollow-core photonic crystal fiber
Gas dynamics
Vacuum

ABSTRACT

The unique design of hollow-core photonic crystal fibers (HC-PCFs) has attracted a lot of researchers' attention. Their hollow-core structure with low transmission loss allow strong light-gas interaction inside the fiber, making HC-PCF a strong candidate as portable gas cells for sensing or spectroscopic purposes. Gas-filled HC-PCFs also have applications in the study of Raman scattering (SRS) transient regime and waveguides research. Considering the design of the cell, it is important to understand the gas flow dynamic, for example, estimate the evacuation or gas filling time for a certain length of fiber. In this paper, the gas dynamics theory and the comparison between single- and double-end pumping in special HC-PCFs is investigated. For two different types of HC-PCFs, our experimental data verified the trend for pressure decrease during the evacuation process was consistent with the theoretical prediction. After adding a correction factor, which represents the hollow-core structure of the fiber, to the existing model, the simulation results matched well with the experimental observation.

1. Introduction

Since the advent of hollow-core photonic crystal fibers (HC-PCF) [1,2], they have been attracting a lot of attention due to many interesting properties [3–6]. Their unique design of hollow-core structure with low transmission loss allows strong light-gas interaction inside the fiber. The interaction between light and gas can be further enhanced by increasing the fiber length. Based on these advantages, it has been proposed that hollow-core PCF (HC-PCF) can be used to fabricate HC-PCF gas cell [7–25], which has a wide range of applications in the fields of spectral absorption [7,8], optical fiber sensing [9–13], and laser frequency stabilization [14–16]. Important light-matter interactions in HC-PCFs also include the excitation and effective generation of optical rogue waves [29] and the importance of transient regime in gas-filled HC-PCFs [26–29]. Monfared et al. investigated different propagation regimes of stimulated Raman scattering (SRS) in gas-filled HC-PCFs [27]. Nazarkin et al. suggested the possibilities that gas-filled HC-PCFs offer a broad spectrum for controlling nonlinear interactions based on SRS in the gas phase [28]. Among various types of HC-PCFs, microstructured fiber (MSF) and suspended-core fiber (SCF) have many important applications. For example, MSF is useful to serve as a gas inlet for fiber-based gas pressure sensors [30]. SCF is widely used in the manufacture of gas sensors. A fast-response mid-infrared gas sensor [31] and a high-resolution fiber-optic ultrasonic sensor based on a suspended-core fiber [32] were reported.

HC-PCF-based gas cells generally have two categories depending on the gas pressure sealed inside the fiber: high-pressure and low-pressure gas cells. At present, many researches prefer low-pressure cell because it can largely reduce the spectral broadening for the absorption line width due to high gas pressure and thus achieve a high spectral resolution [14]. Meanwhile, one has to use long fiber length to compensate the reduced absorption strength. Problem arises when using long HC-PCFs. For example, the gas inflation process

* Corresponding author.
E-mail address: wushun@wit.edu.cn (S. Wu).

https://doi.org/10.1016/j.ijleo.2021.167797
Received 22 May 2021; Received in revised form 8 August 2021; Accepted 9 August 2021
Available online 12 August 2021

can be days long for meters of HC-PCF. Due to the small size of hollow-cores in HC-PCF, it is important to understand the gas pressure along the fiber at different filling time. For gas sensing applications, the reaction time between the light and gas determines the measurement time of the sensor. The study of the reaction time also requires analysis of the aerodynamic process in the gas sensing chamber.

In the past, Hoo et al. used to observe the change in absorption strength for the acetylene absorption spectroscopy to monitor the gas filling process in hollow-core photonic crystals [6]. However, they were not able to determine the pressure in the fiber core for a certain place along the fiber at a specific time. Based on the optical fiber dynamics theory, Henningsen et al. simulated the time--dependent changes of pressure in the HC-PCF under free molecular flow and hydrodynamic flow [6]. Nevertheless, a drawback in their model is that the HC-PCF with complicated hollow microstructure was simplified to be a capillary tube. On this basis, Wang et al. investigated the pressure characteristics inside the HC-PCF during the evacuation process, specifically, when the system is in two different states: the free molecular flow state and the hydrodynamic flow state. They also calculated the normalized pressure as a function of time for the central position, as well as both ends of the HC-PCF, under single-end pumping and double-end pumping [14]. Parmar et al. established a theoretical model of methane gas diffusion in the hollow cores, and compared the relationship between the gas diffusion time and the fiber length under different pressures [17]. Recently, the gas flow dynamics in a relatively long HC-PCF-based gas sensor was numerically and experimentally investigated [18]. The gas diffusion time and response time are related to the geometric factor determined by the microstructure of that particular HC-PCF. However, none of these articles discuss how different microstructures affect the evacuation and gas-filling performance.

In this paper, we established relevant theoretical models based on Ref. [6], and analyzed different types of HC-PCFs based on the microtube theory [6]. Specifically, we estimated the time for evacuation and inflating dry nitrogen gas for two types of HC-PCFs: MSF and SCF, providing theoretical guidance of fabricating HC-PCF gas cells for spectroscopic and fiber sensing applications.

2. Theory

We aim to establish a model that can simulate the pressure change in a piece of HC-PCF fiber during the gas filling and evacuating process, so that we can estimate the filling time and thus analysis the dynamics of gas flow in the HC-PCF at various positions along the fiber. The theory mostly follows the model in Ref. [6] except that we introduce a *correction factor* K_q, considering the unique microstructure for each HC-PCF.

The pressure gradient drives the homogeneous gas to flow in the fiber core. The specific flow characteristics are determined by the value of Knudsen number:

$$Kn \equiv \lambda/d, \tag{1}$$

λ is defined as the average free path of the collision between molecules and d is the core diameter. Three different fluid regimes are determined according to the value of Kn: free molecular flow, hydrodynamic flow and slip flow, as shown in Fig. 1.

In order to directly compare the evacuation status for different flow regimes, we introduce several dimensionless parameters: dimensionless time, normalized position and pressure. The dimensionless time $t_f$means the proportion of real-time to total time that is required to approach a specific pressure. The normalized pressure ($\kappa = p/p_0$) is defined as the ratio of the real-time pressure to the initial pressure, while the normalized position is defined as the relative position compared to total fiber length. Fig. 2 depicts the change of normalized pressure at different position in the fiber at different dimensionless time in the case of single-end pumping.

From Fig. 2, we can observe the general trend is that for single-end pumping (or filling), the pressure variation on one end is always larger than the other end. Thus, we can believe that for two-ends pumping (or filling), the pressure at both ends of the fiber changes faster than at the center. In addition, as the pumping time increases, the pressure in the cavity decreases nonlinearly and gradually approaches vacuum state. During the filling process, the pressure in the cavity increases nonlinearly and slowly reaches equilibrium.

3. Experimental setup

The experimental system we used to test the HC-PCFs includes a dry nitrogen gas cylinder, a vacuum chamber with two fiber inlets, a few valves and gas lines, as shown in Fig. 3. Two vacuum gauges with different measurement ranges are utilized to read the pressure inside the chamber. They are purchased from Kurt J. Lesker (KJLC615TCK), and Reborn (ZJ-2Y) with measurement range of 1 mTorr $\sim$ 2 Torr (0.13–263 Pa), and 100 Pa $\sim$ 100 kPa, respectively. Both probes of the pressure gauges are installed close to the fiber end inside the chamber. The pumping rate for the mechanical pump is 3 L/s, which allows the sealed chamber to be evacuated to a background pressure at Pascal level. Gas flow can be controlled by the ball valves in the gas line. With the help of the speedy valve in the evacuation line, the chamber can be filled with dry nitrogen at any desired pressure up to one atmosphere.

Depending on whether single-end or two-end pumping or filling is tested, either one or two ends of the HC-PCF are connected to the chamber. A tight seal between the fiber and the steel chamber is realized by pressurizing a rubber ring around the fiber. An initial

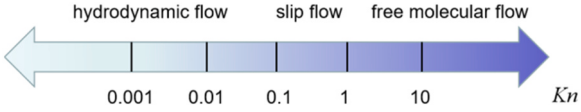

Fig. 1. Different flow regimes determined by the value of Knudsen number.

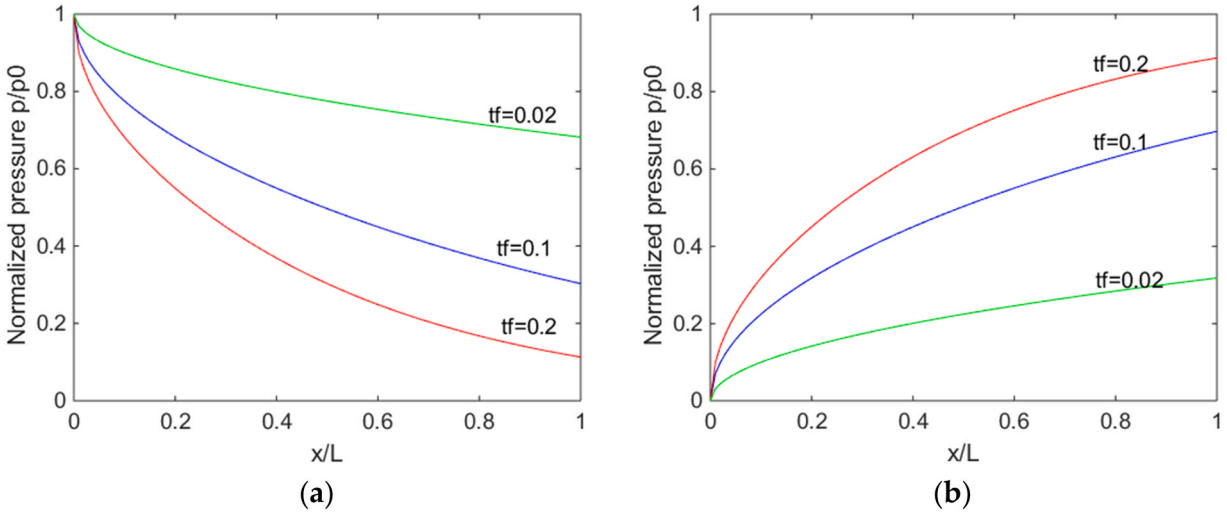

Fig. 2. In the free molecular flow, the normalized pressure changes according to the normalized position during the (a) Pumping process, and (b) Filling process at three different dimensionless times (t_f).

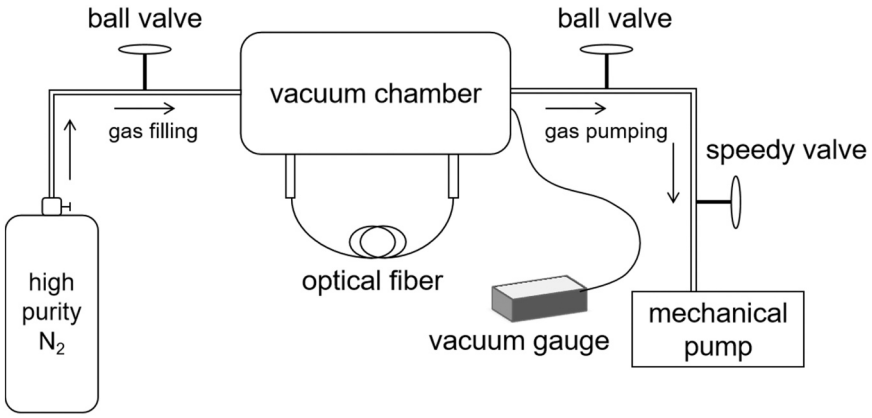

Fig. 3. The principle diagram of the experimental setup.

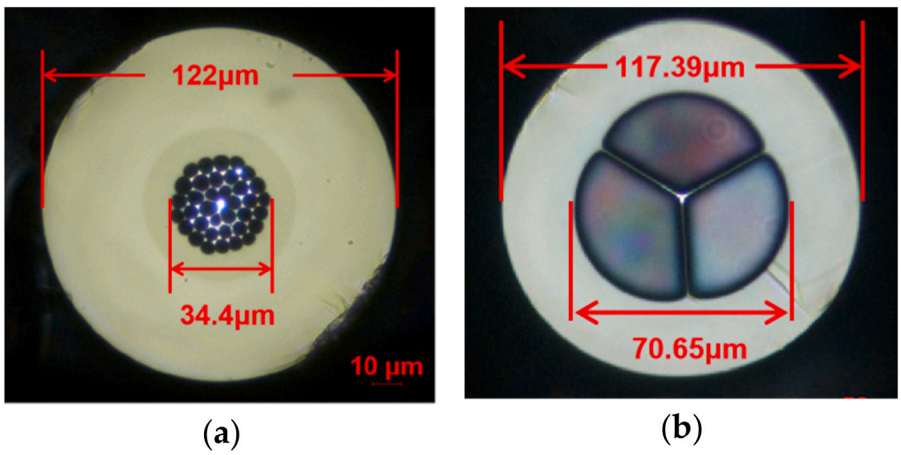

Fig. 4. Cross section of two types of HC-PCFs. (a) Microstructure PCF with core diameter of 34.4 μm, and length of 3.5 m, each individual tube has diameter of 5.8 μm; (b) Suspended-core fiber with core diameter of 70.65 μm, and length of 5.2 m.

vacuum leakage test shows that when both ends of HC-PCF are connected to the chamber, the background pressure can reach equilibrium of a few Pascal or so (8.0 mtorr) after overnight evacuation. The outgas test afterward indicates that with the evacuation line shut off, the pressure inside the sealed chamber increases at a rate of 0.12 mtorr/min (0.0158 Pa/min) for the first hour. This value slowly reaches 0.28 mtorr/min (0.037 Pa/min) in the next 12 h. These results confirm that the chamber has low leakage and good long-term stability, which is essential for the experiments.

Fig. 4 is the microscopic picture for cross section of the two different kinds of HC-PCF we tested in the experiment. In Fig. 4(a), the dark circular area in the center represents the hollow air-cores, while other places are made of fused silica. The suspended-core fiber shown in Fig. 4(b) has three large air-holes in the center with thin glass walls in between two adjacent holes.

4. Results and discussion

We first tested the evacuation process for the hollow-core microstructure PCF shown in Fig. 4(a). Specifically, we measured both the single-end and double-end evacuation time, starting from an initial pressure of one atmosphere. Fig. 5 shows the simulation results using the theory in Ref. [6], the venting pressure is a function of normalized pressure over time as shown in the equation below [3]:

$$F_{vent} = \frac{8}{\pi^2}\sum_{\mu=0}^{\infty}\frac{\exp\{-(2\mu+1)^2\pi^2 t_f\}}{(2\mu+1)^2} \tag{2}$$

Here, t_f is dimensionless time related to real time through the scale factor K_f, real time.

$$t = \frac{3L^2}{\langle v\rangle d}t_f \equiv K_f t_f \tag{3}$$

v is the average velocity $\langle v\rangle = \sqrt{8kT/\pi m}$. L, d and m are the fiber's length, core diameter and molecular mass of the gas, respectively. From Eq. (3), we can see that different molecular gas will affect the average velocity of the molecules and further influence the pumping time.

We simulate the evacuation process for different lengths of microstructure PCFs according Eq. (2). The results are shown in Fig. 5 (a), while the influence of core diameter on evacuation time are illustrated in Fig. 5(b). There is a clear trend that the pressure in the fiber decreases exponentially with time, and the required pumping time increases as the length of the fiber changes from 3 to 10 m and the core diameter is reduced from 60 to 30 μm.

Fig. 6 shows the measured pressure at various evacuation times for double-end and single-end pumping, represented by the open circles and triangles, respectively. The blue dash and red dotted curve represent the corresponding fitting curve for the experimental data. The experimental results verified that the measured pressure at the end of the fiber decreases exponentially as a function of evacuation time in pumping cases, which agrees with the simulation in Fig. 2. We can see that the blue dashed line always stays below that of the red dotted line, indicating that a higher pumping efficiency for double-end than single-end evacuation. In addition, Fig. 6 also represents the comparison between the experimental data and theoretical simulation described in Ref. [6]. In the simulation, we consider the microstructure in HC-PCF as a hollow tube with the same size as the hollow-core area. However, the calculated result, shown as the upper red solid curve in Fig. 6, has large discrepancy from our measurement data, indicated by the hollow symbols. Therefore, we modified our model by treating the process as multiple small tubes being evacuated simultaneously. In Eq. (3), we used the diameter of an individual tube as d, and multiplied by 36, which is the number of individual tubes. The modified simulation curve is shown as the solid green line in Fig. 6, with some improvement compared to the red solid line.

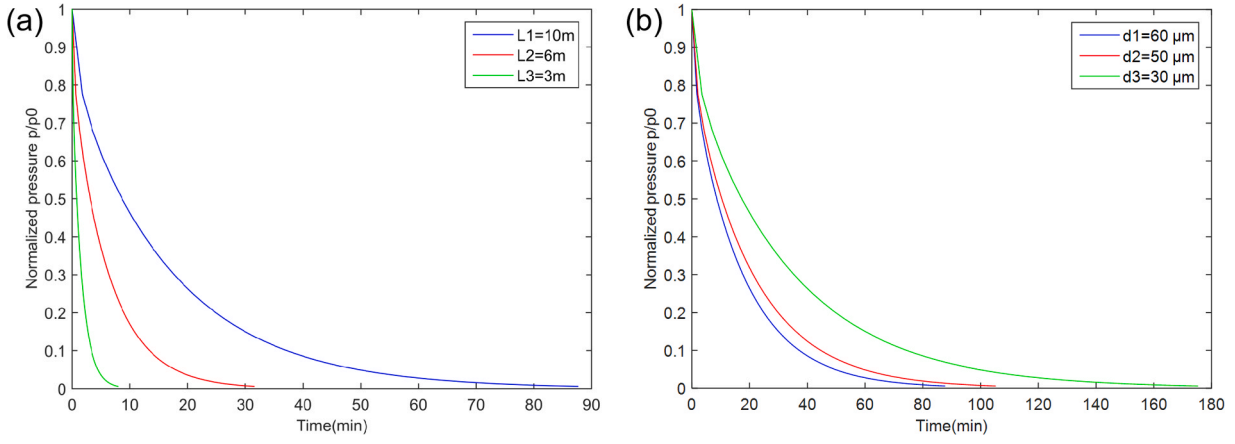

Fig. 5. Theoretical simulation pumping curves for the microstructure PCF in Fig. 4(a). Evacuation time for (a) different lengths, L1 = 10 m, L2 = 6 m, L3 = 3 m, and (b) different core diameters, d1 = 60 μm, d2 = 50 μm, d3 = 30 μm.

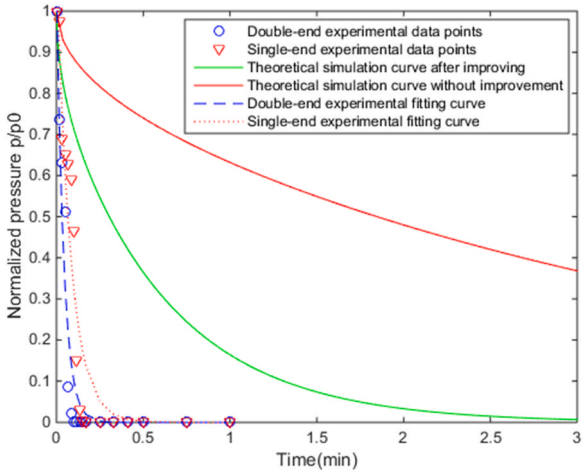

Fig. 6. Single-end and double-end pumping process's comparison with theoretical simulation results without correction factor for the microstructure PCF in Fig. 4(a). For interpretation of the references to color in this figure legend, the reader is referred to the web version of this article.

To solve the discrepancy issue between the calculation and the experimental fitting curve, we introduced a correction factor K_q of 0.01376 for the microstructure PCF in our model and modified Eq. (2):

$$F_{improve} = K_q \cdot F_{vent} = K_q \cdot \frac{8}{\pi^2} \sum_{\mu=0}^{\infty} \frac{\exp\{-(2\mu+1)^2 \pi^2 t_f\}}{(2\mu+1)^2} \tag{4}$$

The value of K_q is calculated to be 0.01376 for the microstructure PCF. The corrected simulation curve is shown as the black solid line in Fig. 7(a), which agrees better with the experimental double-end evacuation fitting curve.

Following the above method, we tested the variation of pressure in the suspended-core fiber (cross-section shown in Fig. 4(b)) for single-end and double-end pumping process. The open circles and triangles are the experimental data for double- and single-end evacuation, respectively, with the blue dash and the red dotted curve as the corresponding fitting curve. The trend of both curves is consistent with the theoretical simulation. The evacuation efficiency for single-end pumping is slower than double-end pumping. Using the aforementioned method, we get a correction factor K_q which value is 0.01895 for the suspended-core fiber.The black solid line represents the corrected simulation result.

We also studied the effect of initial pressure on the pumping rate for the two types of HC-PCF in Fig. 4. Fitting curves are shown in Fig. 8. We can see that the fitting curves are consistent: the low pressure fitting curve stays slightly above the high pressure fitting curves, however, with large uncertainty. This may because the pressure difference between the maximum and minimum pressure under test are not large enough to exhibit clear difference in the evacuation time.

5. Conclusions

Compared with the traditional absorption cell, the HC-PCF gas cell has the advantages of long working distance, small additional loss, and stability. It is widely used in the fields of spectral absorption, fiber sensor, laser frequency stabilization and etc. In this paper, we performed simulation for the pressure changes for two different types of HC-PCFs during the evacuation and filling process. For both fibers, our experimental results showed that the pressure in the cavity decreases exponentially with time, which agreed well with the theoretical prediction. The evacuation time is related to the length of the fiber, the diameter as well as the initial pressure inside the cavity. In order to solve the large discrepancy between the simulation and the experimental data, we added a correction factor to the existing model. The corrected simulation results showed obvious improvement than before. The fact that our preliminary experimental results are consistent with the corrected model provides some insights for understanding the gas dynamics inside hollow-core photonic crystal fibers.

Funding

This research was funded by National Natural Science Foundation of China (NSFC) [grant number 61805182], and Campus Science Foundation of Wuhan Institute of Technology [grant number 18QD19].

Declaration of Competing Interest

The authors declare no conflict of interest.

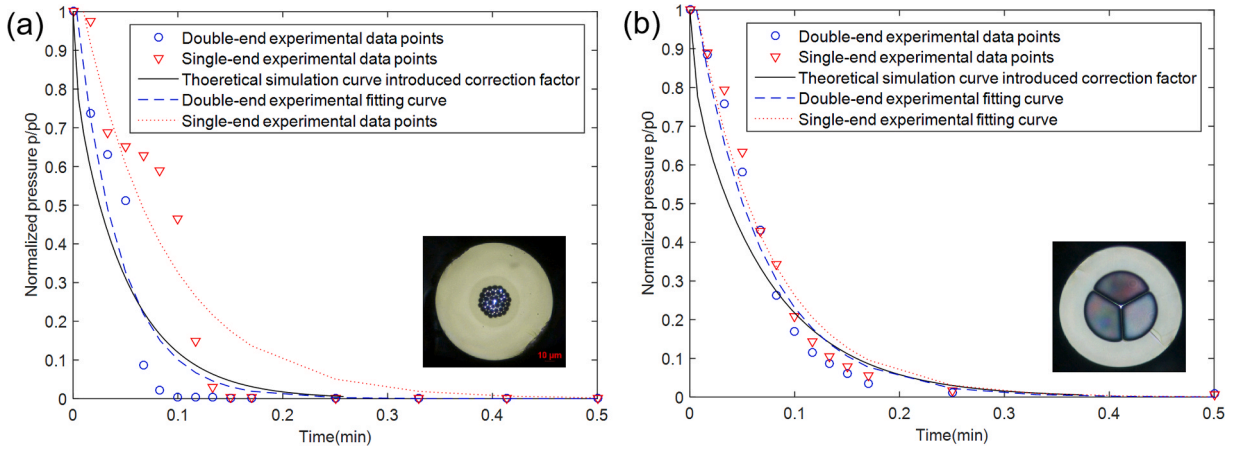

Fig. 7. Comparison between single- and double-end pumping curves respectively for the microstructure PCF and suspended-core fiber in Fig. 4 with theoretical simulation curve after adding correction factor. For interpretation of the references to color in this figure legend, the reader is referred to the web version of this article.

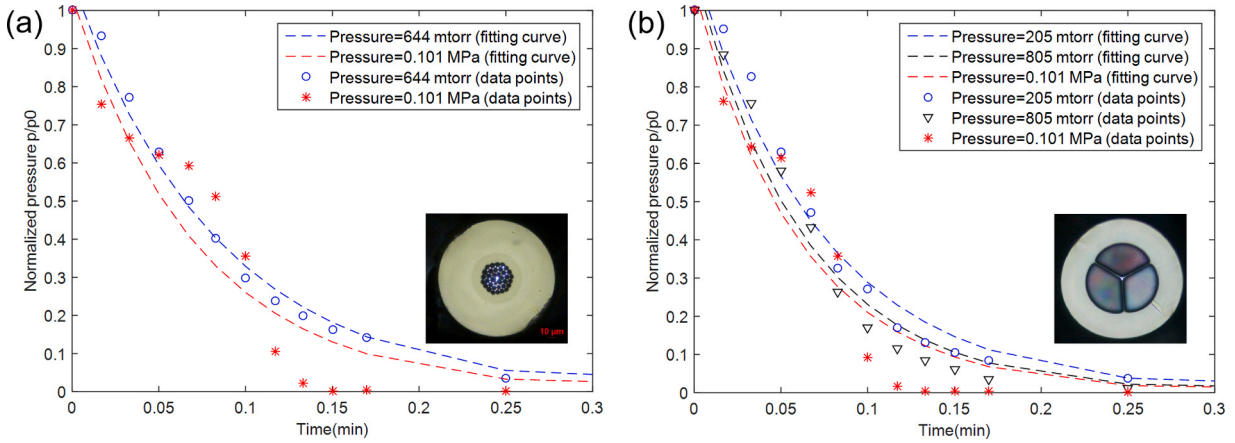

Fig. 8. Experimental pumping curves under different initial pressure for (a) microstructure PCF and (b) suspended-core fiber.

Acknowledgments

We acknowledge Zhuojun Yang and Jiuxing Yan for their earlier contribution to the vacuum setup.

References

[1] J.C. Knight, T.A. Birks, P.S.J. Russell, D.M. Atkin, All-silica single-mode optical fiber with photonic crystal cladding, Opt. Lett. 21 (19) (1996) 1547–1549.
[2] J.C. Knight, J. Broeng, T.A. Birks, P. Russell, Photonic band gap guidance in optical fibers, Science 282 (5393) (1998) 1476–1478.
[3] C. Markos, J.C. Travers, A. Abdolvand, B.J. Eggleton, O. Bang, Hybrid photonic-crystal fiber, Rev. Mod. Phys. 89 (4) (2017), 045003.
[4] Y. Hoo, W.J, H. Ho, J. Ju, D. Wang, Gas diffusion measurement using hollow-core photonic bandgap fiber, Sens. Actuators B 105 (2005) 183–186.
[5] Shun Wu, Haihao Cheng, Jianwen Ma, Xuemei Yang, Shun Wang, Peixiang Lu, Temperature-independent ultra-sensitive refractive index sensor based on hollow-core silica tubes and tapers, Opt. Express 29 (7) (2021) 10939–10948.
[6] Jes Henningsen, Jan Hald, Dynamics of gas flow in hollow core photonic bandgap fibers, Appl. Opt. 47 (15) (2008) 2790–2797.
[7] F. Benabid, J.C.K, P.S.J. Russell, Stimulate Rarran scattering in hydrogen-filled hollow-core photonic crystal fiber, Science 298 (5592) (2002) 399–402.
[8] X.D. Chen, Q.H. Mao, Q. Sun, J.S. Zhao, P. Li, S.J. Feng, An all-fiber gas raman light source based on a hydrogen-filled hollow-core photonic crystal fiber pumped with a Q-switched fiber laser, Chin. Phys. Lett. 28 (7) (2011), 074201.
[9] Jianwen Ma, Shun Wu, Haihao Cheng, Xuemei Yang, Shun Wang, Peixiang Lu, Sensitivity-enhanced temperature sensor based on encapsulated S-taper fiber Modal interferometer, Optics Laser Techno. 139 (2021), 106933.
[10] Xuemei Yang, Shun Wu, Haihao Cheng, Jianwen Ma, Shun Wang, Shuhui Liu, Peixiang Lu, Simplified highly-sensitive gas pressure sensor based on harmonic Vernier effect, Opt. Laser Technol. 140 (2021), 107007.
[11] R. Yu, Y. Chen, L. Shui, L. Xiao, Hollow-core photonic crystal fiber gas sensing, Sensors 20 (2020) 2996.
[12] N. Song, Y. Zhu, X. Xu, S. Xu, F. Gao, Experimental study of hollow-core photonic crystal fiber optical switching effect in liquid nitrogen environment, IEEE Photonics J. 12 (3) (2020), 7101806.
[13] J. Hald, J. Petersen, J. Henningsen, Saturated optical absorption by slow molecules in hollow-core photonic band-gap fibers, Phys. Rev. Lett. 98 (21) (2007), 213902.

[14] Wang Haibin. Development of HC-PCF Low-pressure Gas Cavity for Laser Frequency Stabilization, Anhui Institute of Optics and Fine Mechanics, Chinese Academy of Sciences, 2013.
[15] J. Tuominen, T.R, H. Ludvigsen, J.C. Petersen, Gas filled photonic bandgap fibers as wavelength references, Opt. Commun. 255 (2005) 272–277.
[16] P.T. Marry, J. Morel, T. Feurer, All-fibers frequency-stabilized erbium doped ring laser, Opt. Express 18 (26) (2010) 26821–26827.
[17] Vinod Parmar, R.B, Analysis of gas flow dynamics in hollow core photonic crystal fibre based gas cell, Optik 125 (2014) 3204–3208.
[18] B.M. Masum, S.M. Aminossadati, M.S. Kizil, C.R. Leonardi, Numerical and experimentalinvestigationsof pressure-driven gas flow in hollow-corephotonic crystal fibers, Appl. Opt. 58 (4) (2019) 963–972.
[19] N.V. Wheeler, M.D.W. Grogan, P.S. Light, F. Couny, T.A. Birks, F. Benabid, Large-core acetylene-filled photonic microcells made by tapering a hollow-core photonic crystal fiber, Opt. Lett. 35 (11) (2010) 1875–1877.
[20] T. Ritari, J. Tuominen, H. Ludvigsen, J.C. Petersen, H.R. Simonsen, Gas sensing using air-guiding photonic bandgap fibers, Opt. Express 12 (2004) 4080–4087.
[21] R. Thapa, K. Kabe, K.L. Corwin, B.R. Washburn, Arc fusion splicing of hollow-core photonic bandgap fibers for gas-gilled fiber cell, Opt. Express 14 (21) (2006) 9576–9583.
[22] A.M. Cubillas, J.M. Lazaro, M. Silva-Lopez, O.M. Conde, M.N. Petrovich, J.M. Lopez-Higuera, Methane sensing at 1300nm band with hollow-core photonic band-gap fiber as gas cell, Electron. Lett. 44 (6) (2008) 403–404.
[23] A.M. Cubillas, M. Silva-lopez, J.M. Lazaro, O.M. Conde, J.M. Lopez-Higuera, Methane detection at 1670-nm band using a hollow-core photonic bandgap fibre and a multiline algorithm, Opt. Express 15 (26) (2007) 17570–17576.
[24] J. Henningsen, J. Hald, J.C. Petersen, Saturated absorption in acetylene and hydrogen cyanide in hollow-core photonic band gap fibers, Opt. Express 13 (26) (2005) 10475–10482.
[25] Y. Hoo, W. Jin, H.L. Ho, D.N. Wang, Measurement of gas diffusion coefficient using photonic crystal fiber, IEEE Photon. Tecnol. Lett. 15 (2003) 1434–1436.
[26] Thai Doan Thanh, Ho QuangQuy, Nguyen Manh Thang, Coherent Raman scattering interaction in hydrogen gas-filled hollow core photonic crystal fibres, Optik 161 (2018) 156–160.
[27] Y.E. Monfared, Transient dynamics of stimulated Raman scattering in gas-filled hollow-core photonic crystal fibers, Adv. Mater. Sci. Eng. 2018 (2018), 8951495.
[28] A. Nazarkin, A. Abdolvand, P. St.J. Russell, Optimizing anti-Stokes Raman scattering in gas-filled hollow-core photonic crystal fibers, Phys. Rev. A 79 (2009), 031805.
[29] Yashar E. Monfared, Sergey A. Ponomarenko, Non-Gaussian statistics and optical rogue waves in stimulated Raman scattering, Opt. Express 25 (2017) 5941–5950.
[30] Xuimei Yang, Yongqi Li, Songyang Zhang, Shun Wang, Shun Wu, Comparison of fiber-based gas pressure sensors using hollow-core photonic crystal fibers, Photonics J. 13 (2021), 6800209.
[31] L. Wang, W. Ma, P. Zhang, L. Zhu, D. Yang, X. Wang, S. Dai, Mid-infrared gas detection using a chalcogenide suspended-core fiber, J. Light. Technol. 37 (2019) 5193–5198.
[32] Zhihua Shao, Qiangzhou Rong, Fengyi Chen, Xueguang Qiao, High-spatial-resolution ultrasonic sensor using a micro suspended-core fiber, Opt. Express 26 (2018) 10820–10832.